Accepted Manuscript

Title: A Dynamic Optimization Framework for Integration of Design, Control and Scheduling of Multi-product Chemical Processes under Disturbance and Uncertainty

Authors: Robert W. Koller, Luis A. Ricardez-Sandoval

PII: S0098-1354(17)30206-5
DOI: http://dx.doi.org/doi:10.1016/j.compchemeng.2017.05.007
Reference: CACE 5809

To appear in: *Computers and Chemical Engineering*

Received date: 1-2-2017
Revised date: 3-5-2017
Accepted date: 10-5-2017

Please cite this article as: Koller, Robert W., & Ricardez-Sandoval, Luis A., A Dynamic Optimization Framework for Integration of Design, Control and Scheduling of Multi-product Chemical Processes under Disturbance and Uncertainty.*Computers and Chemical Engineering* http://dx.doi.org/10.1016/j.compchemeng.2017.05.007

A Dynamic Optimization Framework for Integration of Design, Control and Scheduling of Multi-product Chemical Processes under Disturbance and Uncertainty

Robert W. Koller, *Luis A. Ricardez-Sandoval

Dept. of Chemical Engineering, University of Waterloo, Waterloo, ON, Canada N2L 3G1

*Correspondence concerning this article should be addressed to Luis Ricardez-Sandoval at laricard@uwaterloo.ca.

Highlights:

- An algorithm for integration of design, control, and scheduling is proposed.
- Variable transition times are considered using flexible finite elements.
- The proposed algorithm provides a robust solution, superior to the sequential method.
- Interactions between design, control, and scheduling are shown to be significant.
- Multi-product CSTR case study shows the benefits of the algorithm.

Abstract: A novel dynamic optimization framework is presented for integration of design, control, and scheduling for multi-product processes in the presence of disturbances and parameter uncertainty. This framework proposes an iterative algorithm that decomposes the overall problem into flexibility and feasibility analyses. The flexibility problem is solved under a critical (worst-case) set of disturbance and uncertainty realizations, whereas the feasibility problem evaluates the dynamic feasibility of each realization, and updates the critical set accordingly. The algorithm terminates when a robust solution is found, which is feasible under all identified scenarios. To account for the importance of grade transitions in multiproduct processes, the proposed framework integrates scheduling into the dynamic model by the use of flexible finite elements. This framework is applied to a multi-product continuous stirred-tank reactor (CSTR) system subject to disturbance and parameter uncertainty. The proposed method is shown to return robust solutions that are of higher quality than the traditional sequential method. The results indicate that scheduling decisions are affected by design and control decisions, thus motivating the need for integration of these three aspects.

Keywords: dynamic optimization; optimal design and control; process scheduling; decomposition algorithm

1. Introduction

Multiproduct processes are widely used in different sectors due to their versatility and convenience, e.g. oil & gas (Harjunkoski et al., 2009), pharmaceutical (Nie and Biegler, 2012), and polymer production (Harjunkoski et al., 2009; Terrazas-Moreno et al., 2008). To remain competitive, companies are required to operate their systems at nearby optimal conditions that can efficiently produce their products under environmental, safety and product specification constraints. Most major chemical companies have invested in large computing networks that are dedicated to solving large-scale process optimization problems (Seferlis and Georgiadis, 2004). Obtaining a solution for design, control, and scheduling can be quite challenging, as the problems are typically very large, and there are many aspects to a process which can impact the process economics. There are multiple approaches for obtaining solutions, each of which vary in solution quality and computational time.

The simplest approach to address optimal process design, scheduling and control for large process networks is the sequential approach, where the design, control, and scheduling of the system are all considered separately (Patil et al., 2015; Zhuge and Ierapetritou, 2012). This approach is popular in many industries (Mohideen et al., 1996) because solutions can be obtained very quickly, due to independence of the sub-problems. Although the sequential method is fast, there are many limitations. Since each sub-problem is solved independently, the interactions between design, control, and scheduling are typically neglected, even though it has been recognized that these interactions can be significant (Flores-Tlacuahuac and Grossmann, 2011; Pistikopoulos and Diangelakis, 2015; Zhuge and Ierapetritou, 2012). Furthermore, assumptions need to be made in each sub-problem, e.g. steady-state operation or adding overdesign factors, and these assumptions may be invalid or return expensive plant designs. Hence, the solution generated by the sequential approach is likely to be suboptimal, and may become dynamically infeasible in some cases leading to the specification of invalid designs and scheduling sequences (Chu and You, 2014a). These limitations have motivated the development of a more reliable and robust method of determining design, control, and scheduling.

The simultaneous approach is a more advanced method of integrated optimization. In this approach, the design, control, and scheduling are optimized simultaneously, for the purpose of considering interactions. This approach has the potential to provide attractive solutions, which are more optimal and reliable (Chu and You, 2014b; Mendez et al., 2006; Nie et al., 2015; Patil et al., 2015). While several studies have considered integration of design and control (Ricardez-Sandoval et al., 2009; Sakizlis et al., 2004; Yuan et al., 2012), integration of scheduling has not been deeply explored. In the case of multi-product

plants, it can be advantageous to account for scheduling decisions at the design stage since it dictates the dynamic transitions between the different products to be produced, which in turn, depend on design and control (Bhatia and Biegler, 1996; Flores-Tlacuahuac and Grossmann, 2011; Pistikopoulos and Diangelakis, 2015). For large-scale problems, the simultaneous method has a high computational cost due to the large number of variables involved, including the integer variables considered in the scheduling formulation. The problem can be complicated further by considering dynamic evolution of the system subject to process disturbances and uncertainty in the model parameters. Solving the simultaneous problem explicitly is challenging due to the reasons described above; therefore, decomposition algorithms that account for different aspects of the integration of design, control and/or scheduling have been proposed to arrive at economically attractive solutions (Chu and You, 2013; Heo et al., 2003; Mohideen et al., 1996; Sanchez-Sanchez and Ricardez-Sandoval, 2013; Seferlis and Georgiadis, 2004; Zhuge and Ierapetritou, 2016). Currently, there is no commercial software which is specifically designed to solve these types of problems (Pistikopoulos and Diangelakis, 2015).

Typically, the decomposition algorithm consists of two sub-problems: a flexibility analysis and a feasibility analysis (Sakizlis et al., 2004; Sanchez-Sanchez and Ricardez-Sandoval, 2013; Seferlis and Georgiadis, 2004). In the flexibility sub-problem, a solution is chosen such that total cost is minimized and all constraints are satisfied, subject to a critical set of process disturbances and parameter uncertainty. In the feasibility sub-problem, the solution from the flexibility sub-problem is tested for feasibility at all realizations of disturbance and uncertainty. If the solution is determined to be invalid (i.e. infeasible for one or more realizations), the critical set is updated, and the algorithm returns to the flexibility problem. The algorithm terminates when all realizations are feasible at the given solution.

As shown in Table 1, previous publications typically focus on either design and control, design and scheduling, or control and scheduling. Due to problem complexity, few publications address the integration of design, control, and scheduling. In one of the first studies, the design, control, and scheduling of a methyl-methacrylate process are optimized simultaneously (Terrazas-Moreno et al., 2008). The scheduling decisions include production order and transition times, which account for process dynamics. The formulation includes uncertainty, as values that are selected from a discrete set. Process disturbances were not considered. In lieu of a closed-loop control scheme, the profile of the manipulated variable was directly obtained from dynamic optimization. In another study (Patil et al., 2015), the integration was applied to multiproduct processes under disturbance and uncertainty. Decisions were made on equipment sizing, steady-state operating conditions, control tuning, production sequence, and transition times between product grades. The total cost was based on the worst-case disturbance frequency, which was identified using frequency response analysis on the linearized process model. One limitation is that the non-linear

process model was linearized, which reduced the complexity of the problem, but introduced approximations to the model behavior and therefore to the resulting solution. A recent work presents the PAROC solution for solving integrated optimization problems, summarizes recent efforts in the subject area, and proposes simultaneous design and operational optimization of heat and power cogeneration units (Pistikopoulos and Diangelakis, 2015).

The objective of this study is to develop a mathematical framework for integrated dynamic optimization of design, control, and scheduling of multiproduct systems under process disturbances and parameter uncertainty. The novelty of this work is that the proposed approach explicitly considers the mechanistic non-linear dynamic process model with disturbances and parameter uncertainty, while most previous works on integrated optimization have disregarded one or more of those aspects. The scheduling sequence and transition times are explicitly accounted for in the dynamic model by the use of orthogonal collocation on finite elements, where the finite elements are allowed to vary in size. This framework has been applied to a multiproduct CSTR, and several scenarios were considered including a comparison of solution quality between the proposed methodology and the sequential approach.

This paper is organized as follows: the next section outlines the problem definition of the general problem that this framework aims to solve, followed by the mathematical representation of the equations involved in the problem. The framework is applied to a CSTR system, the results and benefits are shown, and then conclusions are presented in the final section. The notation used in the study is defined in the nomenclature section of this article.

2. Problem definition

Consider a multiproduct processing unit that operates continuously, alternating production between various grades of a product in a wheel fashion, such as in Fig. 1. A cycle consists of transition and production regions for each product grade, therefore the total number of regions I is twice the number of grades G. During the transition region, the process set-point is changed linearly (in a ramp fashion) to the next set-point, to allow the system to smoothly transition to the new operating conditions. Following each transition region, a production region begins. The production region ends after a fixed time interval for each grade, after which the transition region begins for the next product grade. This process repeats until the demands for all grades have been satisfied. The duration of each region i is denoted as Δt_i. Additionally, since the processing unit is expected to operate continuously in a wheel fashion, the initial conditions in the first region must be equal to the final conditions in the final region, as shown in Fig. 1.

This study assumes that the following are given: the actual process model representing the system's dynamic behavior, model parameters that are known with certainty (e.g. reaction rate constant, inlet flow

rate), the control scheme, the required product grades and amounts to be produced and process constraints. The present study also assumes that mathematical descriptions describing the process disturbances and uncertain parameters are provided. The framework proposed in this work aims to provide a solution that specifies: the optimal equipment sizing, the optimal steady state operating conditions for each product grade, the optimal control scheme tuning parameters, the sequence of grades to be produced, and the transition times between production of each grade. The proposed solution will be dynamically operable in the presence of disturbances and model uncertainty.

3. Problem formulation

This section presents the algorithmic framework that is proposed to address simultaneous design, control, and short-term scheduling of multi-product plants. First, the formal optimization formulation is presented for the conceptual problem. The approximations made to the original formulation are explained next, followed by the decomposition algorithmic framework proposed in this work.

3.1. Conceptual optimization formulation

The explicit formulation to address the integration of design, scheduling, and control is presented in problem (1). The problem aims to minimize the total expected cost of the process $\boldsymbol{z}$, by manipulating design, control, and scheduling decisions, while subject to time-dependent process disturbances, and uncertainty in model parameters. The design variables $\boldsymbol{\kappa}$ consist of equipment design parameters and operating conditions. The control parameters $\boldsymbol{\Lambda}$ consist of controller tuning parameters (e.g. K_c and τ_i). The scheduling variables consist of integer variables $\boldsymbol{\mathcal{B}}$ that determine the production sequence, and continuous variables $\mathbf{\Delta t}$ that determine the duration of each transition region. For simplicity, all these variables will be referred to collectively as the decision variables $\boldsymbol{\mathcal{D}} = \{\boldsymbol{\kappa}, \boldsymbol{\Lambda}, \boldsymbol{\mathcal{B}}, \mathbf{\Delta t}\}$. Note that each of these decisions are independent (i.e. transition durations $\mathbf{\Delta t}$ do not depend on control parameters, but are instead obtained explicitly from optimization).

$$\min_{\boldsymbol{\mathcal{D}}=\{\boldsymbol{\kappa},\boldsymbol{\Lambda},\boldsymbol{\mathcal{B}},\mathbf{\Delta t}\}} \max_{\boldsymbol{\eta}(t),\boldsymbol{\mathcal{P}}} z(\boldsymbol{x}(t), \boldsymbol{u}(t), \boldsymbol{y}(t), \boldsymbol{y}^{sp}(t), \boldsymbol{\eta}(t), \boldsymbol{\mathcal{P}}, \boldsymbol{\kappa}, \boldsymbol{\Lambda}, \boldsymbol{\mathcal{B}}, \mathbf{\Delta t}) \tag{1}$$

$s.t.$

$$\boldsymbol{f}(\boldsymbol{x}(t), \dot{\boldsymbol{x}}(t), \boldsymbol{u}(t), \boldsymbol{y}(t), \boldsymbol{y}^{sp}(t), \boldsymbol{\eta}(t), \boldsymbol{\mathcal{P}}, \boldsymbol{\kappa}, \boldsymbol{\Lambda}, \boldsymbol{\mathcal{B}}, \mathbf{\Delta t}) = \mathbf{0}$$

$$\boldsymbol{g}(\boldsymbol{x}(t), \boldsymbol{u}(t), \boldsymbol{y}(t), \boldsymbol{y}^{sp}(t), \boldsymbol{\eta}(t), \boldsymbol{\mathcal{P}}, \boldsymbol{\kappa}, \boldsymbol{\Lambda}, \boldsymbol{\mathcal{B}}, \mathbf{\Delta t}) \leq \mathbf{0}$$

$$\boldsymbol{h}(\boldsymbol{x}(t), \boldsymbol{u}(t), \boldsymbol{y}(t), \boldsymbol{y}^{sp}(t), \boldsymbol{\eta}(t), \boldsymbol{\mathcal{P}}, \boldsymbol{\kappa}, \boldsymbol{\Lambda}, \boldsymbol{\mathcal{B}}, \mathbf{\Delta t}) = \mathbf{0}$$

$$\boldsymbol{y}^{sp}(t) = \boldsymbol{\psi}(\boldsymbol{\mathcal{B}}, \mathbf{\Delta t})$$

$$\boldsymbol{\eta}_{lo} \leq \boldsymbol{\eta}(t) \leq \boldsymbol{\eta}_{up}$$

$$\boldsymbol{\mathcal{P}}_{lo} \leq \boldsymbol{\mathcal{P}} \leq \boldsymbol{\mathcal{P}}_{up}$$

$$\boldsymbol{\mathcal{D}}_{l} \leq \boldsymbol{\mathcal{D}} \leq \boldsymbol{\mathcal{D}}_{u}$$

$$\boldsymbol{\mathcal{B}} \in \mathbb{Z}$$

$$t \in [0, t_{end}]$$

The process states $\boldsymbol{x}(t)$ and its derivatives $\dot{\boldsymbol{x}}(t)$ are typically described by differential equations and are represented here by the closed-loop process model $\boldsymbol{f}$. The process constraints can take the form of inequality constraints $\boldsymbol{g}$ (physical constraints, safety constraints, quality constraints, stability constraints, and scheduling constraints) or equality constraints $\boldsymbol{h}$ (typically representing the process model algebraic equations). As shown in problem (1), the output set-points $\boldsymbol{y^{sp}}(t)$ are determined from the integer scheduling decisions $\boldsymbol{\mathcal{B}}$ and the lengths of each time region $\boldsymbol{\Delta t}$ using the function $\boldsymbol{\psi}$. The vector of process disturbances $\boldsymbol{\eta}(t)$ is time-varying but is assumed to be bounded by a lower limit $\boldsymbol{\eta}_{lo}$ and an upper limit $\boldsymbol{\eta}_{up}$ whereas the vector of uncertain parameters $\boldsymbol{\mathcal{P}}$ is assumed to be time-invariant and bounded by a lower limit $\boldsymbol{\mathcal{P}}_{lo}$ and an upper limit $\boldsymbol{\mathcal{P}}_{up}$. The conceptual formulation shown in problem (1) can be considered as a robust optimization formulation given that the optimal solution is required to remain valid at the worst-case critical realizations of process disturbances and parametric uncertainty, thus resulting in a minimax optimization problem. Also, the formulation presented in problem (1) makes no assumptions about the disturbances and the uncertain parameters, i.e. $\boldsymbol{\eta}(t)$ and $\boldsymbol{\mathcal{P}}$ are assumed to be continuous variables encompassing an infinite number of possible realizations. Therefore, problem (1) can be classified as an infinite-dimensional mixed integer non-linear dynamic optimization problem. A large-scale problem of this type is very challenging to solve for many reasons, notably the infinite search space for disturbance and uncertain parameter domains, the combination of scheduling (integer) and continuous decisions, and the corresponding solution of differential equations at each step in the optimization. This provides motivation for the development of efficient algorithms that can circumvent these difficulties, and make the problem tractable.

3.2. Decomposition Algorithm

In this section, the assumptions used to make the bulk problem (1) tractable are explained. The time domain is discretized, reformulating all continuous variables into discrete points. Following that, the approximations for process disturbances and parameter uncertainty are presented. The decomposition algorithm is explained, along with each of the sub-problems.

3.2.1. Discretization of time domain

The problem under consideration includes time-dependent variables, which are embedded within the closed-loop dynamic model of the system defined by the vector function $\boldsymbol{f}$. In addition, integer variables $\boldsymbol{\mathcal{B}}$ are considered in the analysis to account for scheduling decisions. Thus, presence of these time-dependent and integer variables makes the overall problem a mixed-integer nonlinear dynamic optimization (MIDO) problem. These types of problems can be solved using two approaches; the shooting method, and the simultaneous method. In the shooting method, the ODEs are solved at fixed levels of the decision variables, and this is repeated multiple times in a sensitivity analysis to calculate the gradients of the objective and constraints. The gradients are then used to update the decision variables, and the process is repeated. In the simultaneous method, the ODEs are discretized, reformulating the differential equations as algebraic equations, which are then implemented into a bulk model along with the decision variables. More details about the shooting method and the simultaneous method can be found elsewhere (Biegler, 2010). The analytical gradients can be determined, and an optimal solution can be approached. In this work, the simultaneous approach has been used to reduce the computational costs and facilitate the integrated optimization of design, control, and scheduling decisions. Accordingly, the ODEs representing the closed-loop dynamic equations $\boldsymbol{f}$ are transformed into algebraic form using orthogonal collocation on finite elements, resulting in an overall problem that is a mixed-integer non-linear program (MINLP). As shown in Fig. 2, the time domain is divided into I regions, which alternate between transition regions and production regions. Each region contains J finite elements, and each finite element contains K collocation points which are spaced according to Gauss-Legendre quadrature. The duration of each region i (Δt_i) is directly determined from optimization, allowing for differently sized regions to be explicitly accounted for in the MINLP formulation. As the size of each region i changes, the size of the contained finite elements (δt_i), and their collocation points, also changes. In each region i, the size of finite elements δt_i is related to the total region size Δt_i as shown in Eq. 2.

$$\Delta t_i = J \delta t_i \quad \forall i \tag{2}$$

Based on the above descriptions, the process states $\boldsymbol{x}(t)$ can be discretized and defined as $\boldsymbol{x}_{ijk}$, as shown in Eq. 3, where i is the index of time regions, j is the index of finite elements, and k is the index of collocation points. The remaining time-dependent variables (i.e. $\boldsymbol{y^{sp}}(t)$, $\boldsymbol{u}(t)$, $\boldsymbol{\eta}(t)$ etc.) and functions (i.e. $\boldsymbol{g}$, $\boldsymbol{h}$) are discretized in the same fashion. The value of time at each point is a function of i, j, k and the region lengths $\boldsymbol{\Delta t}$. Moreover, the time derivative for process states $\dot{\boldsymbol{x}}(t)$ can be discretized using the orthogonal collocation matrix $\boldsymbol{\mathcal{A}}$, which is defined in Appendix A, and the finite element size δt_i in each region i. Furthermore, the time-dependent variables are defined using two more indices (θ, ω), where θ and ω are the indexes corresponding to particular realizations in parameter uncertainty, and process disturbances, respectively.

$$\dot{\boldsymbol{x}}(t) = \boldsymbol{f}(\boldsymbol{x}(t), \boldsymbol{y^{sp}}(t), \boldsymbol{u}(t), \boldsymbol{\eta}(t), \boldsymbol{\mathcal{P}}) \rightarrow \sum_{k'} \boldsymbol{\mathcal{A}}_{kk'} \boldsymbol{x}_{ijk'}^{\theta,\omega} = \delta t_i \, \boldsymbol{f}\left(\boldsymbol{x}_{ijk}^{\theta,\omega}, (\boldsymbol{y}^{sp})_{ijk}, \boldsymbol{u}_{ijk}^{\theta,\omega}, \boldsymbol{\eta}_{ijk}^{\omega}, \boldsymbol{\mathcal{P}}^{\theta}\right)$$
$$i \in \{1,2,\dots,I\}, j \in \{1,2,\dots,J\}, k \in \{1,2,\dots,K\} \quad \omega \in \{1,2,\dots,N\}, \theta \in \{1,2,\dots,M\} \tag{3}$$

As shown in problem (1), the region lengths $\boldsymbol{\Delta t}$ (i.e. transition and production durations) are decision variables in the optimization. The effect of scheduling on the model equations can be seen directly in Eq. (3), which includes the finite element size δt_i for each region i directly in the process model. Also, Eq. (3) depends on the set-points of the system at each discrete point in time i, j, k (i.e. $(\boldsymbol{x}^{sp})_{ijk}$), where the corresponding set-points imposed on the process at any time point i, j, k are determined from the function $\boldsymbol{\psi}$, which depends on the binary sequencing matrix $\boldsymbol{\mathcal{B}}$ and the region lengths $\boldsymbol{\Delta t}$, i.e. scheduling decisions. The process to obtain $(\boldsymbol{x}^{sp})_{ijk}$ is described in detail in Appendix B. This represents a novelty in the present formulation since scheduling decisions are explicitly accounted for in the optimal design and control of multi-product systems under the effect of disturbances and uncertainty; an aspect that, to the authors' knowledge, has not been addressed in the literature.

To ensure zero- and first-order continuity between regions, and between finite elements, additional constraints are added to the formulation, i.e.

$$\boldsymbol{x}_{i,j,K}^{\theta,\omega} = \boldsymbol{x}_{i,j+1,1}^{\theta,\omega} \quad \forall i,j \wedge \forall(\theta,\omega) \in \boldsymbol{c} \tag{4}$$
$$\boldsymbol{x}_{i,J,K}^{\theta,\omega} = \boldsymbol{x}_{i+1,1,1}^{\theta,\omega} \quad \forall i \wedge \forall(\theta,\omega) \in \boldsymbol{c} \tag{5}$$
$$\frac{\sum_{k'} \mathcal{A}_{K,k'} \boldsymbol{x}_{i,j,k'}^{\theta,\omega}}{\delta t_i} = \frac{\sum_{k'} \mathcal{A}_{1,k'} \boldsymbol{x}_{i,j+1,k'}^{\theta,\omega}}{\delta t_i} \quad \forall i,j \wedge \forall(\theta,\omega) \in \boldsymbol{c} \tag{6}$$
$$\frac{\sum_{k'} \mathcal{A}_{K,k'} \boldsymbol{x}_{i,J,k'}^{\theta,\omega}}{\delta t_i} = \frac{\sum_{k'} \mathcal{A}_{1,k'} \boldsymbol{x}_{i+1,1,k'}^{\theta,\omega}}{\delta t_{i+1}} \quad \forall i \wedge \forall(\theta,\omega) \in \boldsymbol{c} \tag{7}$$

3.2.2. Process Disturbances and Parameter Uncertainty Descriptions

As shown in the conceptual problem (1), the process disturbances $\boldsymbol{\eta}(t)$ have been initially defined as bounded time-varying continuous variables, which makes problem (1) computationally challenging. To circumvent this issue, the present analysis approximates the disturbances from a set of possible functions specified *a priori*, as shown in Eq. (8). For example, the set of disturbances can take the form of sinusoidal waves with different frequency content (i.e. variability). The index ω refers to the particular realization that the disturbance can take during operation; e.g. the frequency for a sinusoidal disturbance. Similarly, the vector of uncertain parameters $\boldsymbol{\mathcal{P}}$ are approximated from a set of possible realizations defined *a priori*. The index θ refers to the particular realization that the parameter uncertainty vector $\boldsymbol{\mathcal{P}}$ can take during operation, as shown in Eq. (9). The realizations corresponding to $\omega = 0$ or $\theta = 0$ represent the nominal operating

condition considered for those parameters. The sets of realizations for disturbance and uncertainty should be selected carefully, as different sets will affect the solution provided by the framework. Note that increasing the number of discrete realizations is expected to have a diminishing effect on the solution (i.e. the problem is expected to converge to the same solution as the number of scenarios grows sufficiently large).

$$\boldsymbol{\eta}_{ijk}^{\omega} \in \left\{\boldsymbol{\eta}_{ijk}^{0}, \boldsymbol{\eta}_{ijk}^{1}, \boldsymbol{\eta}_{ijk}^{2}, \dots, \boldsymbol{\eta}_{ijk}^{N}\right\} \quad \forall\, i,j,k \qquad \omega \in \{0,1,2,\dots,N\} \tag{8}$$

$$\boldsymbol{\mathcal{P}}^{\theta} \in \{\boldsymbol{\mathcal{P}}^{0}, \boldsymbol{\mathcal{P}}^{1}, \boldsymbol{\mathcal{P}}^{2}, \dots, \boldsymbol{\mathcal{P}}^{M}\} \qquad \theta \in \{0,1,2,\dots,M\} \tag{9}$$

In the present analysis, a critical set $\boldsymbol{c}$ is introduced in Eq. (10) as a set of (ω,θ) pairs. This set is used to define the realizations among those defined in Eq. (8) and (9) that have the most critical impact on process performance, and may also produce dynamic infeasibility. Note that when a realization is referred to as *critical*, it is with respect to the discrete set of disturbance and uncertain realizations, which are defined *a priori*. Each set of pairs in $\boldsymbol{c}$ is a subset of all combinations of (ω,θ) considered in the disturbance and uncertain parameter sets, i.e. all (N×M) combinations.

$$\boldsymbol{c} \subseteq \omega \times \theta = \begin{bmatrix} (0,0) & \cdots & (0,M) \\ \vdots & \ddots & \vdots \\ (N,0) & \cdots & (N,M) \end{bmatrix} \tag{10}$$

3.2.3. Algorithm Formulation

Using the approximations described above, the conceptual problem (1) can be transformed into a minimax MINLP. Furthermore, to avoid the challenging task of optimizing over every possible combination of (ω,θ) in an MINLP problem, a decomposition algorithm is implemented. As shown in Fig. 3, the proposed algorithm decomposes the problem into a Flexibility Analysis and a Feasibility Analysis. These sub-problems contain the actual process model and nonlinear constraints (in discrete form), and also include orthogonal collocation constraints, Eq. (4)-(7), which are required to ensure continuity of the process state variables $\boldsymbol{x}_{ijk}^{\theta,\omega}$ and their derivatives due to the discretization scheme employed in this work.

The flexibility analysis formulation is presented in problem (11). This problem is initialized with a critical set $\boldsymbol{c}$, which specifies the realizations of process disturbances $\boldsymbol{\eta}_{ijk}^{\omega}$ and parameter uncertainty $\boldsymbol{\mathcal{P}}^{\theta}$ to be considered in the analysis. As shown in Fig. 3, the critical set can be initialized in the first iteration ($n=1$) with the corresponding nominal values (i.e. $\boldsymbol{\eta}_{ijk}^{0}$, $\boldsymbol{\mathcal{P}}^{0}$). For a fixed critical set $\boldsymbol{c}$, the flexibility analysis searches for the design, control, and scheduling scheme that minimizes the expected cost in the objective function and accommodates the realizations considered in critical set $\boldsymbol{c}$. As shown in problem (11), each

critical realization is weighted by a user-defined factor $\zeta^{\theta,\omega}$, which must be defined *a priori* and represents the likelihood or confidence that realization (θ,ω) may occur during operation.

$$\min_{\boldsymbol{\mathcal{D}}=\{\boldsymbol{\kappa},\boldsymbol{\Lambda},\boldsymbol{\mathcal{B}},\boldsymbol{\Delta t}\}} \sum_{(\theta,\omega)\in\boldsymbol{c}} \zeta^{\theta,\omega} z^{\theta,\omega}\left(\boldsymbol{x}_{ijk}^{\theta,\omega}, \boldsymbol{y}_{ijk}^{\theta,\omega}, (\boldsymbol{y}^{sp})_{ijk}, \boldsymbol{\kappa}, \boldsymbol{\Lambda}, \boldsymbol{\mathcal{B}}, \boldsymbol{\Delta t}\right) \tag{11}$$

$s.t.$

$$\sum_{k'} \mathcal{A}_{kk'} \boldsymbol{x}_{ijk'}^{\theta,\omega} = \delta t_i \boldsymbol{f}\left(\boldsymbol{x}_{ijk}^{\theta,\omega}, \boldsymbol{u}_{ijk}^{\theta,\omega}, \boldsymbol{y}_{ijk}^{\theta,\omega}, (\boldsymbol{y}^{sp})_{ijk}, \boldsymbol{\eta}_{ijk}^{\omega}, \boldsymbol{\mathcal{P}}^{\theta}, \boldsymbol{\kappa}, \boldsymbol{\Lambda}, \boldsymbol{\mathcal{B}}, \delta t_i\right), \quad \forall i,j,k \wedge \forall(\theta,\omega)\in\boldsymbol{c}$$

$$\boldsymbol{g}\left(\boldsymbol{x}_{ijk}^{\theta,\omega}, \boldsymbol{u}_{ijk}^{\theta,\omega}, \boldsymbol{y}_{ijk}^{\theta,\omega}, (\boldsymbol{y}^{sp})_{ijk}, \boldsymbol{\eta}_{ijk}^{\omega}, \boldsymbol{\mathcal{P}}^{\theta}, \boldsymbol{\kappa}, \boldsymbol{\Lambda}, \boldsymbol{\mathcal{B}}, \delta t_i\right) \leq \boldsymbol{0}, \quad \forall i,j,k \wedge \forall(\theta,\omega)\in\boldsymbol{c}$$

$$\boldsymbol{h}\left(\boldsymbol{x}_{ijk}^{\theta,\omega}, \boldsymbol{u}_{ijk}^{\theta,\omega}, \boldsymbol{y}_{ijk}^{\theta,\omega}, (\boldsymbol{y}^{sp})_{ijk}, \boldsymbol{\eta}_{ijk}^{\omega}, \boldsymbol{\mathcal{P}}^{\theta}, \boldsymbol{\kappa}, \boldsymbol{\Lambda}, \boldsymbol{\mathcal{B}}, \delta t_i\right) = \boldsymbol{0}, \quad \forall i,j,k \wedge \forall(\theta,\omega)\in\boldsymbol{c}$$

$$(\boldsymbol{y}^{sp})_{ijk} = \boldsymbol{\psi}_{ijk}(\boldsymbol{\mathcal{B}}), \quad \forall i,j,k \wedge \forall(\theta,\omega)\in\boldsymbol{c}$$

$$\boldsymbol{\mathcal{D}}_l \leq \boldsymbol{\mathcal{D}} \leq \boldsymbol{\mathcal{D}}_u$$

$$\boldsymbol{\mathcal{B}} \in \mathbb{Z}$$

$Equations\ (4)-(7)$

The optimal solution for design, control, and scheduling returned by the flexibility problem is only guaranteed to be valid for the critical realizations considered in $\boldsymbol{c}$. Thus, a feasibility analysis is needed to ensure a robust solution that is immune to any combination of disturbance and parameter uncertainty. Therefore, the solution from the flexibility problem at the n^{th} iteration ($\boldsymbol{\mathcal{D}}_n$) is held constant and is passed to the feasibility problem. As shown in problem (12), a formal feasibility analysis optimization formulation can be formulated to search for the combination of (ω,θ) in the disturbances and uncertain parameters that produces the maximum (positive) deviation in the slack variables $\boldsymbol{\alpha}$, at any point in time i,j,k, for constraint $g_a \in \boldsymbol{g}$. Binary variables ($Y_{a,ijk}^{\theta,\omega}$) are incorporated into the formulation to identify such a condition. Note that a problem of this type would be very difficult to solve on a continuous time domain with non-discretized disturbance and parameter uncertainty, due to the infinite-dimensional search space, as mentioned in Section 3.1. Active set strategies (Mohideen et al., 1996) and structured singular value analysis (Trainor et al., 2013) have been proposed to solve such problems. The problem in (12) is an integer optimization (IP) problem, as all the decisions are made on binary variables. Although the search space is finite, the problem is challenging to solve directly due to the curse of dimensionality, as the number of integer variables grows prohibitively large. However, the finite search space lends itself very well to rigorous simulations. Recent studies have used simulations to evaluate feasibility (Mansouri et al., 2016; Pistikopoulos et al., 2015; Ricardez-Sandoval, 2012; Shi et al., 2016; Zhuge and Ierapetritou, 2016). In this work, and with the aim of reducing computational complexity, process simulations are performed to calculate the values of the

process variables (e.g. $\boldsymbol{x}_{ijk}^{\theta,\omega}$) and constraint violations $\alpha_{a,ijk}^{\theta,\omega}$, over the entire discrete set of process disturbances and parameter uncertainty, as shown in problem (12A).

$$\phi = \max_{\boldsymbol{Y}} \sum_{a,i,j,k,\theta,\omega} Y_{a,ijk}^{\theta,\omega}\, \alpha_{a,ijk}^{\theta,\omega} \tag{12}$$

$s.t.$

$$\sum_{k'} \boldsymbol{\mathcal{A}}_{kk'} \boldsymbol{x}_{ijk'}^{\theta,\omega} = \delta t_i * \boldsymbol{f}\left(\boldsymbol{x}_{ijk}^{\theta,\omega}, (\boldsymbol{x}^{sp})_{ijk}, \boldsymbol{u}_{ijk}^{\theta,\omega}, \boldsymbol{y}_{ijk}^{\theta,\omega}, \boldsymbol{\eta}_{ijk}^{\omega}, \boldsymbol{\mathcal{P}}^{\theta}, \boldsymbol{\kappa}, \boldsymbol{\Lambda}, \boldsymbol{\mathcal{B}}, \delta t_i\right) \quad \forall\, i,j,k$$

$$g_{a,ijk}^{\theta,\omega}\left(\boldsymbol{x}_{ijk}^{\theta,\omega}, (\boldsymbol{x}^{sp})_{ijk}, \boldsymbol{u}_{ijk}^{\theta,\omega}, \boldsymbol{y}_{ijk}^{\theta,\omega}, \boldsymbol{\eta}_{ijk}^{\omega}, \boldsymbol{\mathcal{P}}^{\theta}, \boldsymbol{\kappa}, \boldsymbol{\Lambda}, \boldsymbol{\mathcal{B}}, \delta t_i\right) = \alpha_{a,ijk}^{\theta,\omega}\,, \quad \forall\, a,i,j,k$$

$$\boldsymbol{h}\left(\boldsymbol{x}_{ijk}^{\theta,\omega}, (\boldsymbol{x}^{sp})_{ijk}, \boldsymbol{u}_{ijk}^{\theta,\omega}, \boldsymbol{y}_{ijk}^{\theta,\omega}, \boldsymbol{\eta}_{ijk}^{\omega}, \boldsymbol{\mathcal{P}}^{\theta}, \boldsymbol{\kappa}, \boldsymbol{\Lambda}, \boldsymbol{\mathcal{B}}, \delta t_i\right) = \boldsymbol{0}\,, \quad \forall\, i,j,k$$

$$\sum_{a,i,j,k,\theta,\omega} Y_{a,ijk}^{\theta,\omega} = 1$$

$$Y_{a,ijk}^{\theta,\omega} \in \{0,1\} \quad \forall\, \theta,\omega,a,i,j,k$$

$$Equations\ (4) - (7)$$

$$\Phi = \max_{\theta,\omega}\ \alpha_{a,ijk}^{\theta,\omega} \tag{12A}$$

$s.t.$

$$\sum_{k'} \boldsymbol{\mathcal{A}}_{kk'} \boldsymbol{x}_{ijk'}^{\theta,\omega} = \delta t_i * \boldsymbol{f}\left(\boldsymbol{x}_{ijk}^{\theta,\omega}, (\boldsymbol{x}^{sp})_{ijk}, \boldsymbol{u}_{ijk}^{\theta,\omega}, \boldsymbol{y}_{ijk}^{\theta,\omega}, \boldsymbol{\eta}_{ijk}^{\omega}, \boldsymbol{\mathcal{P}}^{\theta}, \boldsymbol{\kappa}, \boldsymbol{\Lambda}, \boldsymbol{\mathcal{B}}, \delta t_i\right) \quad \forall\, i,j,k$$

$$g_{a,ijk}^{\theta,\omega}\left(\boldsymbol{x}_{ijk}^{\theta,\omega}, (\boldsymbol{x}^{sp})_{ijk}, \boldsymbol{u}_{ijk}^{\theta,\omega}, \boldsymbol{y}_{ijk}^{\theta,\omega}, \boldsymbol{\eta}_{ijk}^{\omega}, \boldsymbol{\mathcal{P}}^{\theta}, \boldsymbol{\kappa}, \boldsymbol{\Lambda}, \boldsymbol{\mathcal{B}}, \delta t_i\right) = \alpha_{a,ijk}^{\theta,\omega}\,, \quad \forall\, a,i,j,k$$

$$\boldsymbol{h}\left(\boldsymbol{x}_{ijk}^{\theta,\omega}, (\boldsymbol{x}^{sp})_{ijk}, \boldsymbol{u}_{ijk}^{\theta,\omega}, \boldsymbol{y}_{ijk}^{\theta,\omega}, \boldsymbol{\eta}_{ijk}^{\omega}, \boldsymbol{\mathcal{P}}^{\theta}, \boldsymbol{\kappa}, \boldsymbol{\Lambda}, \boldsymbol{\mathcal{B}}, \delta t_i\right) = \boldsymbol{0}\,, \quad \forall\, i,j,k$$

$$\theta \in \{1,2,\dots,M\}$$

$$\omega \in \{1,2,\dots,N\}$$

$$Equations\ (4) - (7)$$

The realization with the highest objective function (i.e. the most infeasible realization) in the feasibility problem is deemed the "worst case" realization for the current iteration of the algorithm, represented as $(\omega,\theta)_n$ as shown in Fig. 3. Associated with that realization is a vector of slack variables $\boldsymbol{\alpha}^{(\omega,\theta)_n}$, where positive values represent infeasible operating conditions. As shown in Problem (12A) and Fig. 3, if $\Phi_n \geq 0$, i.e. any slack variables related to the "worst case" realization $(\omega,\theta)_n$ in iteration n are greater than zero, which implies a dynamically infeasible operation because a constraint g_a is violated, then the algorithm continues to the next iteration, adding the worst case realization $(\omega,\theta)_n$ to

the critical set $\boldsymbol{c}$, and solving the flexibility problem subject to the updated critical set. Conversely, if $\Phi_n \leq 0$, i.e. all the slack variables are less than or equal to zero (i.e. all operating conditions are dynamically feasible), the algorithm terminates, and returns the current solution $\boldsymbol{\mathcal{D}}_n$ to be the most optimal solution $\boldsymbol{\mathcal{D}}^*$. This is a robust solution that is dynamically feasible for all the discrete realizations of disturbance and uncertainty that have been considered; however, it is not guaranteed to be optimal for the entire set of realizations in the disturbance and uncertain parameters. Furthermore, dynamic feasibility cannot be guaranteed for realizations other than at the discrete points in Eq. (8) and (9). Adding more realizations in the disturbances and uncertain parameter sets will improve the robustness of the resulting design, control and scheduling scheme at the expense of solving more intensive and challenging optimization problems. Structural decisions (e.g. control schemes, integer design decisions) can be considered in the flexibility analysis using additional integer variables, at the cost of increased complexity. Though the solution is robust, it may be overly conservative, especially in cases of very rare critical realizations. This can be partially remedied by careful selection of the weights $\zeta^{\theta,\omega}$ for each realization. However, robust solutions always remain conservative to some degree. Current research carried out by the authors is focused on developing new numerical approaches that can reduce the conservatism in the solution.

4. Results and discussions: non-isothermal CSTR

This section describes the case study that was adopted for the application of the methodology described in Section 3. The results presented in this work were obtained using GAMS on a system running Windows 7, using an Intel® Core™ i7-2600 CPU 3.40 GHz and 8.00 GB RAM. For MINLP problems, SBB is the chosen solver. For NLP and CNS (constrained non-linear system), CONOPT is selected. Hence, the present analysis accepts locally optimal solutions. Preliminary analysis showed that these solvers provided better performance than other solvers (e.g. DICOPT, IPOPT) for this case study.

The approach described in the previous section has been applied to a continuous stirred tank reactor (CSTR), which is shown in Fig. 4. This case study is intended to be of similar complexity to the case studies used in other works on integrated design, control and/or scheduling optimization (Mehta and Ricardez-Sandoval, 2016; Patil et al., 2015; Terrazas-Moreno et al., 2008; Zhuge and Ierapetritou, 2016, 2012). The reactor has constant volume, due to an overflow outlet. The reactor is non-isothermal, and is capable of producing multiple grades of product B via an irreversible first-order reaction that coverts reactant A into product B. Demand for each of the grades is assumed to be equal, and they are produced one at a time, i.e. in a wheel fashion. Scheduling decisions include the production sequence and the transition durations (i.e. region lengths $\boldsymbol{\Delta t}$) between product grades. During the production regions, set-point tracking of product concentration is desired.

As shown in Fig. 4, the feed to the reactor consists entirely of species A, at a concentration of $C_{A_{in}}$ ($3.0\ mol/L$), flow rate q_{in}, and temperature T_{in} (40°C). The feed must be converted to product B via an exothermic reaction. The reaction is assumed to follow first order Arrhenius kinetics as in Eq. (13).

$$r_A = k_o C_A \exp\left(\frac{-E_R}{R\,T}\right) \tag{13}$$

where C_A is the concentration of species A in the reactor, k_o is the pre-exponential constant ($1.3\ s^{-1}$), R is the gas constant ($8.3144\ J \cdot mol^{-1} \cdot K^{-1}$), T is the temperature in the reactor, and E_R is the activation energy of the reaction ($20000\ J/mol$). The dynamic behavior of the state variables $\boldsymbol{x}_{CSTR} = \{T, C_B\}$ is described in Eq. (14)-(15). Equations are shown in continuous form and have been discretized before implementation as shown in Section 3. Orthogonal collocation for this case study is discussed further in Appendix A.

$$\frac{dT}{dt} = \frac{q_{in}(T_{in} - T)}{V} + \frac{\Delta H_R k_o (C_{A_{in}} - C_B)}{\rho\, C_P} \exp\left(\frac{-E_R}{R\,T}\right) - \frac{Q_H}{\rho C_P V} \tag{14}$$

$$\frac{dC_B}{dt} = k_o\left(C_{A_{in}} - C_B\right) \exp\left(\frac{-E_R}{R\,T}\right) + \frac{q_{in} C_B}{V} \tag{15}$$

where C_B is the concentration of species B (product) in the reactor, V is the volume of liquid in the reactor, ΔH_R is the heat of reaction ($4780\ J/mol$), ρ is the density of the liquid in the reactor ($1\ kg/L$), C_P is the specific heat capacity of the liquid ($4.1813\ J \cdot g^{-1} \cdot K^{-1}$), and Q_H is the rate at which heat is added/removed to the system.

The control scheme consists of a PI controller that uses the heating rate Q_H to control the product concentration C_B at the outlet. As shown in Eq. (16), the concentration set-point is denoted by C_B^{sp} whereas the controller parameters are represented by the proportional gain K_c, and the integral time τ_i. The steady state (nominal) heating rate is $Q_{H_{SS}}$. Due to large differences between typical values of $C_B(t)$ and $Q_H(t)$, the value of K_c is scaled by 10^6 (not shown), for clarity of results.

$$Q_H(t) = Q_{H_{SS}} + K_C\left(C_B^{sp} - C_B(t)\right) + \frac{K_c}{\tau_i}\int_0^t \left(C_B^{sp} - C_B(t')\right) dt' \tag{16}$$

For safety reasons, the temperature inside the reactor must be maintained between 0°C and 400°C during operation, as shown in Eq. (17). Additionally, the rate of change in the manipulated variable (heat input Q_H) is constrained, as shown in Eq. (18), to prevent drastic changes in the heat input. This case study considers five set-points C_B^{sp} shown in Eq. (19), which are also referred to as set-points A, B, C, D, E respectively. As described in Section 2, for each set-point, there is a corresponding transition and production

region. As such, there are I=10 regions; consisting of 5 production regions and 5 transition regions. As described in Section 3.2.1, all variables are discretized into regions i, finite elements j, and collocation points k. In this case study, each region i contains 100 finite elements, i.e. J=100. Within each finite element, there are K=5 collocation points, including the boundary points. The number of finite elements and collocation points were selected *a priori* based on a preliminary analysis of computational effort against accuracy in the solution.

To account for grade transitions, the duration Δt_i of each region i is an optimization variable in the transition regions (odd numbered regions), and is bounded as shown in Eq. (20) to resemble a real process where there may be scheduling/operational limits imposed on time. In production regions (even numbered regions), the region duration is fixed at 4,000 seconds. As discussed in Section 3.2.3, additional constraints are necessary to ensure zero- and first-order continuity between finite elements and regions. Details on the implementation for this case study are discussed in Appendix A.

$$0°\text{C} \leq T \leq 400°\text{C} \tag{17}$$

$$-50\ \text{kW/s} \leq \frac{dQ_H(t)}{dt} \leq 50\ \text{kW/s} \tag{18}$$

$$C_B^{sp} \in \{0.7, 0.9, 1.2, 1.5, 1.7\}\ L/mol \tag{19}$$

$$10\ s \leq \Delta t_i \leq 300\ s \qquad \forall\ i \mid i \text{ odd} \tag{20}$$

The objective of the optimization problem is to minimize total cost of the process. The total cost z_{CSTR} shown in Eq. (21) is assumed to be the sum of capital cost, scheduling cost, and variability cost. Capital cost is a direct function of reactor volume V, scheduling cost is a function of the length of each transition region Δt_i, and variability cost is a function of the integral of squared error ISE_i of the outlet product concentration in each production region. Gaussian quadrature is used in place of a traditional integral to calculate ISE_i, as shown in (22), where φ_k is the Gaussian weight of each discrete point. Note that the weights assigned to each of the cost function terms were arbitrarily selected.

$$z_{CSTR} = 10V + 20 \sum_{i\ \text{odd}} \Delta t_i + 10 \sum_{i\ \text{even}} ISE_i \tag{21}$$

$$ISE_i = \sum_j \sum_{k \notin \{1,K\}} \frac{\varphi_k}{2} \delta t_i \left(C_{B_{ijk}}^{sp} - C_{B\,ijk} \right)^2 \qquad \forall\ i \tag{22}$$

The decision variables for this case study are the reactor volume V (design decisions), the controller tuning parameters K_C and τ_i (control decisions) and the sequence of production (binary matrix $\boldsymbol{\mathcal{B}}$) and the

transition region lengths $\boldsymbol{\Delta t}$ (scheduling decisions). Constraints on the production sequence such that only one grade is produced at a time (Eq. (23)), and all grades are produced by the end of the time horizon (Eq. (24)) were included in the flexibility analysis formulation. Due to the repeating production schedule as mentioned in Section 2, there are many production sequences which are identical (e.g. A-B-C-D-E and B-C-D-E-A, etc.). Therefore, to reduce the computational costs, the first set-point is fixed so it is always the first grade ($0.7\ mol/L$).

$$\sum_{g'} \mathcal{B}_{g,g'} = 1 \quad \forall g \tag{23}$$

$$\sum_{g} \mathcal{B}_{g,g'} = 1 \quad \forall g' \tag{24}$$

4.2. Scenario A

In this scenario, the results from two implementations are compared. The first problem (*Scenario A1*) considers that the selected process disturbance, i.e. the inlet flow rate q_{in}, is set to its nominal operating condition while the second problem (*Scenario A2*) considers an oscillating inlet flow rate q_{in}. In both problems, design, control, and scheduling are optimized simultaneously using the proposed algorithm. The purpose of this scenario is to illustrate the effect that disturbance has on the optimal design, control, and scheduling.

As shown in Eq. (25), the inlet flow rate q_{in} is assumed to oscillate around a nominal point $q_{in_{nom}}$ (0.4 L/s) following a sinusoidal wave with an amplitude of $q_{in_{amp}}$ (0.08 L/s),. The oscillation frequency Ω is assumed to be an unknown parameter chosen from a discrete set of frequencies shown in Eq. (26). Accordingly, $\omega \in \{0,1,2,\ldots,10\}$ refers to a particular disturbance realization, similar to Eq. (8) in Section 3.2.2. All realizations are assumed to be equally likely, i.e. $\zeta^{\omega} = 1/11$. In *Scenario A1*, the inlet flow rate is assumed to be equal to the nominal value, i.e. $\Omega = 0$.

$$q_{in} = q_{in_{nom}} + q_{in_{amp}} \sin(\Omega t) \tag{25}$$

$$\Omega \in \{0, 0.001, 0.002, 0.004, 0.007, 0.01, 0.02, 0.04, 0.07, 0.1, 0.2\}\ s^{-1} \tag{26}$$

The results for these implementations are summarized in Table 2. *Scenario A1* requires a single flexibility problem to generate a solution subject to nominal conditions. *Scenario A2* requires four iterations of the proposed algorithm to converge to an optimal solution that is feasible for all the realizations considered. Note that the solution provided by *Scenario A1* does not remain feasible under all realizations of process disturbance (not shown for brevity). The size of the flexibility analysis (11) in *Scenario A2* grows

in each successive iteration, because the problem must be solved over all realizations in the critical set, which is expanded following each feasibility analysis, as shown in Fig. 3. In the final iteration of the algorithm for *Scenario A2*, the flexibility problem consisted of 119,529 equations and 89,553 variables, while the feasibility simulations consisted of 21,507 equations and variables. The use of simulations in the feasibility analysis is justified, as the formal optimization in (12) would have contained 50,000 binary variables, resulting in a nearly intractable IP problem. Conversely, the computational time for the feasibility analysis simulations in (12A) required only 25 seconds.

The problem size of *Scenario A1* is smaller than that of *Scenario A2*, consisting of 46,519 equations and 36,543 variables. As expected, the CPU time is much higher for *Scenario A2* (at least one order of magnitude) since the problem is larger and requires multiple iterations. As expected, the total process cost and ISE are higher in *Scenario A2,* due to the presence of disturbance. Note that both scenarios returned different scheduling solutions, in terms of sequencing and transition durations, aside from the starting point (which was fixed). *Scenario A2* has lower transition durations, to account for process disturbances. Control parameters are also significantly different, due to the differences in scheduling. Furthermore, the reactor volume is 13% larger in *Scenario A2* than in *Scenario A1*. These results highlight the importance of taking scheduling decisions into account while performing the optimal design of a multiproduct system. Fig. 5 displays the concentration profile from each of the scenarios. The differences in sequence, transition times, and control tuning can be observed.

4.3. Scenario B

In this scenario, results from the proposed methodology (*Scenario B1*) are compared to the results from the sequential method (*Scenario B2*) and the sequential method with overdesign factors (*Scenario B3*). The purpose of this scenario is to compare these competing methodologies in terms of solution quality and computational time. The problems are solved subject to the process disturbance described in the previous scenario. Additionally, uncertainty is considered for two parameters in this process: heat of reaction ΔH_R, and activation energy E_R. The corresponding value of these parameters is determined by the uncertainty realization $\theta \in \{0,1,2,3,4\}$ as shown in Table 3. Note that the complexity of the problem increases since all the combinations of disturbance (11 realizations) and uncertainty (5 realizations) are considered, resulting in 55 possible realizations. The decomposed algorithm is initialized with $\omega = 0$ (see Eq. (25)) and $\theta = 0$, to represent nominal values.

For *Scenario B2 and B3*, the sequential method consists of three consecutive sub-problems (i.e. design, control, and scheduling), where the solution from each sub-problem is fixed in the calculations and passed to the next sub-problem; hence, there is no interaction between the different sub-problems. Due to

the independence of the sub-problems in the sequential method, it is much less complex than the simultaneous approach. Once a solution is determined using the sequential method, the solution is tested against the full set of realizations of disturbance and uncertainty. The worst-case solution (i.e. the most infeasible solution) is returned as the final solution. This is to provide a fair comparison to the proposed method, which also returns the solution that accommodates the worst-case (critical) realizations in ω and θ. The solution obtained from the sequential approach (*Scenario B2*) contained multiple infeasible realizations. Hence, an overdesign factor of 1.5 was applied to the reactor volume in *Scenario B3* to prevent dynamic infeasibility, based on a preliminary analysis of overdesign factors ranging from 1.1 to 2.0, in increments of 0.05. With the overdesigned sequential approach (*Scenario B3*), all the realizations become feasible and comparison to the integrated approach is possible.

For *Scenario B1*, five iterations of the proposed algorithm are required before convergence is met. Results following the flexibility problem from each iteration are summarized in Table 4. The critical set $\boldsymbol{c}$ is initialized with the nominal point $(0,0)$, and a new realization in the disturbance and uncertain parameters is added to the critical set in each iteration. The effects of the expanding critical set can be seen as the problem size increases and the solution changes slightly in each iteration. Given that the present approach uses the solution from the previous iteration to initialize the problem at the current iteration, then a direct relationship between computational costs and problem size shall not be expected since it also depends on other factors such as initial conditions and non-linearities. In the final iteration, all realizations are identified as feasible in the feasibility analysis, so the algorithm is terminated, and the design, control and scheduling scheme corresponding to that iteration is reported as the optimal solution ($\boldsymbol{\mathcal{D}}^*$) as shown in Fig. 3.

Table 5 presents the results obtained from *Scenario B*. As shown in this table, the optimal process cost provided by the integrated approach (*Scenario B1*) is 17% lower than the solution provided by the overdesigned sequential approach (*Scenario B3*), and every component of the cost function is also lower. *Scenario B2* has the lowest process cost out of all scenarios considered though it returns a dynamically infeasible design. The computational cost of the integrated approach (*Scenario B1*) is approximately three times higher than that of *Scenario B3*, due to the increased complexity of the integrated problem, as mentioned above.

As shown in Table 5, the controller integral time is significantly different for each approach, and the lower variability cost indicates that the integrated approach offers better set-point tracking performance than *Scenario B3*. The reactor volume is also lower in the integrated approach, leading to a 16% lower design cost compared to *Scenario B3*. Note that the reactor volume from the integrated approach (V = 18.9) is only 26% greater than *Scenario B2* (V = 15), which was found to be dynamically infeasible. This indicates that by integrating design with control and scheduling decisions, the reactor volume was able to remain

relatively low without resulting in dynamically infeasible (invalid) designs in the presence of disturbance and parameter uncertainty. Additionally, it is likely that reactor volume has a large effect on process dynamics; thus, the reactor sizing in the sequential approach is suboptimal because it is determined in the first stage of optimization (before control and scheduling have been determined). Note that the production sequence and transition durations are also significantly different. This is a clear indication that scheduling decisions are affected by design and control decisions, thus motivating the need for integration of these three aspects. *Scenario B1* and *Scenario B3* are feasible over all realizations of process disturbance and uncertainty, while *Scenario B2* is dynamically infeasible. The concentration profiles from *Scenario B1* and *Scenario B3* are shown in Fig. 6, where differences can be observed in production sequence, transition times, process variability and controller tuning.

In Fig. 7a, it can be observed that the temperature from the integrated approach (*Scenario B1*) remains within the corresponding limits specified for this variable (see Eq. (17)), and oscillates as closely as possible to the limit. For *Scenario B2*, the temperature surpasses the upper bound, resulting in infeasible operating conditions. In Fig. 7b, the profile of the manipulated variable (heat input) in *Scenario B1* is illustrated. Similar to temperature, the heat input oscillates to correct for changes in the disturbances and the uncertain parameters (ΔH_R and E_R), and no drastic changes are observed.

The progression of the algorithm in the integrated approach can be observed in Fig. 8, which displays the maximum infeasibility (Φ_n) detected from the feasibility analysis at each iteration n. Infeasibility starts out high (55 °C above upper bound), and then generally decreases with each iteration, although that is not guaranteed. The algorithm terminates after the fifth iteration, when no infeasibilities were detected, i.e. $\Phi \leq 0$.

4.4. Scenario C

In this scenario, a sensitivity analysis is performed on the weights in the objective function (Eq. 21) to determine the effect on the solution. The case study is the same as described in *Scenario B*. Three scenarios are considered in this section. *Scenarios C1, C2* and *C3* have a 10% increase in the capital cost weight, the scheduling cost weight and the variability cost weight, respectively. To simplify the analysis, each scenario is initialized with the solution from *Scenario B1*. As shown in Table 6, the three scenarios returned a solution that is nearly identical to that obtained for *Scenario B1* with only very small differences in transition times and controller integral time. For *Scenarios C1*, *C2* and *C3,* a change in the total process cost of 3.03%, 1.81% and 5.11%, respectively, is observed with respect to that obtained from *Scenario B1*. These differences in the total process cost are fully explained by the differences in cost weights, i.e. a 10% increase in the capital cost weight returned a 10% increase in the capital cost for *Scenario C1*. Similar

observations can be drawn for *Scenarios C2* and *C3*. These results show that the solutions obtained for the present case study are robust (i.e. insensitive) to small changes in the weights specified in the cost function.

5. Conclusions

A framework for integration of design, control, and scheduling for multiproduct processes under disturbance and uncertainty has been presented. The novelty of this framework is that it performs a direct integration of design, control, and scheduling, while explicitly accounting for scheduling decisions in the process model by the use of variable-sized finite elements in the model discretization. The decomposition algorithm successfully simplifies the problem of an infinite-dimensional search space over all disturbance and uncertainty, by considering a critical set of disturbance and uncertainty, greatly reducing the computational costs. This method is specifically for multiproduct processes, due to the scheduling formulation. However, it can be extended to consider other processes where scheduling is key, e.g. flow-shop systems.

The framework was applied to a case study of a multiproduct CSTR. It is shown that design, control, and scheduling are affected by one another, and it can be advantageous to optimize them simultaneously. The results from the integrated approach are compared to the common alternative, the sequential method. The proposed integrated approach is able to return a solution in a practical time frame, with improved feasibility and optimality compared to the sequential method. The improvement in solution quality, and the tractable computational time required by the proposed methodology shows that it can be a promising approach for integrated optimization of design, control, and scheduling. This framework can be extended to more complex case studies, such as flow-shop systems or multi-product plug flow reactors, although the effect on computational time still needs to be investigated.

6. Acknowledgement

The authors would like to acknowledge the financial support provided by the Natural Sciences & Engineering Council of Canada (NSERC) and the Ontario Graduate Scholarship (OGS).

References

Bhatia, T., Biegler, L., 1996. Dynamic optimization in the design and scheduling of multiproduct batch plants. Ind. Eng. Chem. Res. 5885, 2234–2246. doi:10.1021/ie950701i

Biegler, L.T., 2010. Nonlinear Programming: Concepts, Algorithms, and Applications to Chemical Processes. doi:10.1137/1.9780898719383

Chu, Y., You, F., 2014a. Model-based integration of control and operations: Overview, challenges, advances, and opportunities. Comput. Chem. Eng. 83, 2–20. doi:10.1016/j.compchemeng.2015.04.011

Chu, Y., You, F., 2014b. Integrated Planning , Scheduling , and Dynamic Optimization for Batch Processes : MINLP Model Formulation and Efficient Solution Methods via Surrogate Modeling. Ind. Eng. Chem. Res. 53, 13391–13411.

Chu, Y., You, F., 2013. Integration of scheduling and dynamic optimization of batch processes under uncertainty: Two-stage stochastic programming approach and enhanced generalized benders decomposition algorithm. Ind. Eng. Chem. Res. 52, 16851–16869. doi:10.1021/ie402621t

Flores-Tlacuahuac, A., Grossmann, I.E., 2011. Simultaneous cyclic scheduling and control of tubular reactors: Parallel production lines. Ind. Eng. Chem. Res. 50, 8086–8096. doi:10.1021/ie101677e

Harjunkoski, I., Nyström, R., Horch, A., 2009. Integration of scheduling and control-Theory or practice? Comput. Chem. Eng. 33, 1909–1918. doi:10.1016/j.compchemeng.2009.06.016

Heo, S., Lee, K., Lee, H., Lee, I., Park, J.H., 2003. A New Algorithm for Cyclic Scheduling and Design of Multipurpose Batch Plants. Am. Chem. Soc. 836–846.

Mansouri, S.S., Sales-Cruz, M., Huusom, J.K., Gani, R., 2016. Systematic integrated process design and control of reactive distillation processes involving multi-elements. Chem. Eng. Res. Des. 115, 348–364. doi:10.1016/j.cherd.2016.07.010

Mehta, S., Ricardez-Sandoval, L. a., 2016. Integration of Design and Control of Dynamic Systems under Uncertainty: A New Back-Off Approach. Ind. Eng. Chem. Res. 55, 485–498. doi:10.1021/acs.iecr.5b03522

Mendez, C.A., Cerda, J., Grossmann, I.E., Harjunkoski, I., Fahl, M., 2006. State-of-the-art review of optimization methods for short-term scheduling of batch processes. Comput. Chem. Eng. 30, 913–946. doi:10.1016/j.compchemeng.2006.02.008

Mohideen, M.J., Perkins, J.D., Pistikopoulos, E.N., 1996. Optimal design of dynamic systems under uncertainty. AIChE J. 42, 2251–2272. doi:10.1002/aic.690420814

Nie, Y., Biegler, L.T., 2012. Integrated Scheduling and Dynamic Optimization of Batch Processes Using State Equipment Networks. AIChE J. 58, 3416–3432. doi:10.1002/aic

Nie, Y., Biegler, L.T., Villa, C.M., Wassick, J.M., 2015. Discrete time formulation for the integration of scheduling and dynamic optimization. Ind. Eng. Chem. Res. 54, 4303–4315. doi:10.1021/ie502960p

Patil, B.P., Maia, E., Ricardez-Sandoval, L., 2015. Integration of Scheduling, Design, and Control of Multiproduct Chemical Processes Under Uncertainty. AIChE J. 61, 2456–2470. doi:10.1002/aic

Pistikopoulos, E.N., Diangelakis, N.A., 2015. Towards the integration of process design, control and scheduling: Are we getting closer? Comput. Chem. Eng. 91, 85–92. doi:10.1016/j.compchemeng.2015.11.002

Pistikopoulos, E.N., Diangelakis, N.A., Oberdieck, R., Papathanasiou, M.M., Nascu, I., Sun, M., 2015. PAROC—An integrated framework and software platform for the optimisation and advanced model-based control of process systems. Chem. Eng. Sci. 136, 115–138. doi:http://dx.doi.org/10.1016/j.ces.2015.02.030

Ricardez-Sandoval, L.A., 2012. Optimal design and control of dynamic systems under uncertainty: A probabilistic approach. Comput. Chem. Eng. 43, 91–107. doi:10.1016/j.compchemeng.2012.03.015

Ricardez-Sandoval, L.A., Budman, H.M., Douglas, P.L., 2009. Integration of design and control for chemical processes: A review of the literature and some recent results. Annu. Rev. Control 33, 158–171. doi:10.1016/j.arcontrol.2009.06.001

Sakizlis, V., Perkins, J.D., Pistikopoulos, E.N., 2004. Recent advances in optimization-based simultaneous process and control design. Comput. Chem. Eng. 28, 2069–2086. doi:10.1016/j.compchemeng.2004.03.018

Sanchez-Sanchez, K., Ricardez-Sandoval, L., 2013. Simultaneous Process Synthesis and Control Design under Uncertainty: A Worst-Case Performance Approach. AIChE J. 59, 2497–2514. doi:10.1002/aic

Seferlis, P., Georgiadis, M.C., 2004. The Integration of Process Design and Control, Computer-Aided Chemical Engineering. Elsevier Ltd.

Shi, J., Biegler, L.T., Hamdan, I., 2016. Optimization of grade transitions in polyethylene solution polymerization processes. Comput. Chem. Eng. 62, 1126–1142. doi:10.1002/aic.15113

Terrazas-Moreno, S. and, Flores-Tlacuahuac, A., Grossmann, I.E., 2008. Simultaneous Design, Scheduling, and Optimal Control of a Methyl-Methacrylate Continuous Polymerization Reactor. AIChE J. 54, 3160–3170. doi:10.1002/aic

Trainor, M., Giannakeas, V., Kiss, C., Ricardez-Sandoval, L.A., 2013. Optimal process and control design under uncertainty: A methodology with robust feasibility and stability analyses. Chem. Eng. Sci. 104, 1065–1080. doi:10.1016/j.ces.2013.10.017

Yuan, Z., Chen, B., Sin, G., Gani, R., 2012. State-of-the-Art and Progress in the Optimization-based Simultaneous Design and Control for Chemical Processes. AIChE J. 58, 1640–1659. doi:10.1002/aic

Zhuge, J., Ierapetritou, M.G., 2016. A Decomposition Approach for the Solution of Scheduling Including Process Dynamics of Continuous Processes. Ind. Eng. Chem. Res. 55, 1266–1280. doi:10.1021/acs.iecr.5b01916

Zhuge, J., Ierapetritou, M.G., 2012. Integration of scheduling and control with closed loop implementation. Ind. Eng. Chem. Res. 51, 8550–8565. doi:10.1021/ie3002364

Appendix A. Orthogonal Collocation on Finite Elements for CSTR case study

In orthogonal collocation on finite elements, each finite element is divided into a number of collocation points. In this work, the number of collocation points is 5. One benefit of orthogonal collocation is that the derivative $\dot{\boldsymbol{x}}$ can be estimated from the values $\boldsymbol{x}$ at each collocation point, as shown in (A.1). The matrix entries $\mathcal{A}_{k,k'}$ defines the weighting that each point k' has towards the derivative at point k, and is defined in (A.2) using the Lagrange polynomial $\ell_{k'}(r_k)$ in (A.3), where the roots $\boldsymbol{r}$ are analogous to dimensionless time within each finite element, and are defined as the roots of the Legendre polynomial which lie within [0,1]. For finite elements of non-unit lengths, the derivative must be scaled using δt_i, as in (A.1).

$$\dot{\boldsymbol{x}}_{ijk} = \frac{\sum_{k'} \mathcal{A}_{kk'} \boldsymbol{x}_{ijk'}}{\delta t_i} \quad \forall\, i,j,k \tag{A.1}$$

$$\mathcal{A}_{kk'} = \frac{\partial \ell_{k'}(r_k)}{\partial r} \quad \forall\, k,k' \tag{A.2}$$

$$\ell_{k'}(r_k) = \prod_{\substack{k''=1,\\ k''\neq k'}}^{K} \frac{r_k - r_{k''}}{r_{k'} - r_{k''}} \quad \forall\, k,k' \tag{A.3}$$

The model in the case study (Section 4) is discretized into indices i,j,k. The number of regions I is required to be 10, in order to be double the number of product grades, which is 5. The number of finite elements J is selected to be 100 to allow for long production times of one hour, and to provide a reasonable balance between speed and accuracy. The number of collocation points K is selected to be 5 to allow for a fourth-order polynomial approximation.

In the case study, to ensure zero- and first-order continuity of $\boldsymbol{x}_{CSTR}$, for $\boldsymbol{x}_{CSTR} = \{T, C_B\}$, (A.4) through (A.15) must be included in the problem formulation. These equations are analogous to the general form shown in Section 3.2.1 as Eq. (4)-(7), except here they are shown expanded and in discrete form, exactly as they are implemented.

$$C_{B\,i,j,5} = C_{B\,i,j+1,1} \qquad \forall i,j \tag{A.5}$$

$$C_{B\,i,100,5} = C_{B\,i+1,1,1} \quad \forall i \tag{A.6}$$

$$\frac{\sum_{k'} \mathcal{A}_{5,k'} C_{B\,i,j,k'}}{\delta t_i} = \frac{\sum_{k'} \mathcal{A}_{1,k'} C_{B\,i,j+1,k'}}{\delta t_i} \qquad \forall i,j \tag{A.7}$$

$$\frac{\sum_{k'} \mathcal{A}_{5,k'} C_{B\,i,100,k'}}{\delta t_i} = \frac{\sum_{k'} \mathcal{A}_{1,k'} C_{B\,i+1,1,k'}}{\delta t_{i+1}} \quad \forall i \tag{A.8}$$

$$T_{i,j,5} = T_{i,j+1,1} \quad \forall i,j \tag{A.9}$$

$$T_{i,100,5} = T_{i+1,1,1} \quad \forall i \tag{A.10}$$

$$\frac{\sum_{k'} \mathcal{A}_{5,k'} T_{i,j,k'}}{\delta t_i} = \frac{\sum_{k'} \mathcal{A}_{1,k'} T_{i,j+1,k'}}{\delta t_i} \quad \forall i,j \tag{A.11}$$

$$\frac{\sum_{k'} \mathcal{A}_{5,k'} T_{i,100,k'}}{\delta t_i} = \frac{\sum_{k'} \mathcal{A}_{1,k'} T_{i+1,1,k'}}{\delta t_{i+1}} \quad \forall i \tag{A.12}$$

Appendix B. Set-point Determination from Binary Sequence Matrix

In the problem formulations, the function $\boldsymbol{\psi}_{ijk}$ maps the binary matrix $\boldsymbol{\mathcal{B}}$ to a profile of set-points $\boldsymbol{y}_{ijk}^{sp}$ $\forall\, i,j,k$. Within the binary matrix $\boldsymbol{\mathcal{B}}$, element $\mathcal{B}_{g,g'}$ indicates if set-point $\mathrm{Y}_{g'}^{sp}$ is being produced g^{th} in the sequence. Note that the index of grades g is a subset of the index of time regions i, so some values of i may be used as the index for $\mathcal{B}_{g,g'}$ or β_g, in place of g. The list of set-points $\mathbf{Y}^{\mathrm{sp}}$ is known *a priori*. Linear transitions between set-points are applied during transition regions (odd-numbered regions). As mentioned in Appendix A, $\boldsymbol{r}$ represent the roots of the Legendre polynomial which lie within [0,1].

$$\boldsymbol{\psi}_{ijk}(\boldsymbol{\mathcal{B}}) = \begin{Bmatrix} \beta_G + (\beta_1 - \beta_G)(j - 1 + r_k) & for\ i = 1 \\ \beta_{i/2} & for\ i = 2,4,6, \dots\ I \\ \beta_{\frac{i-1}{2}} + \left(\beta_{\frac{i+1}{2}} - \beta_{\frac{i-1}{2}}\right)(j - 1 + r_k) & for\ i = 3,5,7, \dots (I-1) \end{Bmatrix} \forall\, j,k \tag{B.1}$$

$$where\ \beta_g = \sum_{g'} \mathcal{B}_{g,g'}\, \mathrm{Y}_{g'}^{sp} \quad \forall g$$

Nomenclature:

Indices:

g = index of product grades $(1,2,\dots,G)$

i = index of production/transition regions in time $(1,2,\dots,I)$

j = index of finite elements in time $(1,2,\dots,J)$

k = index of collocation points in time $(1,2,\dots,K)$

ω = index of realizations for process disturbances $(1,2,\dots,N)$

θ = index of realizations for parameter uncertainty $(1,2,\dots,M)$

a = index of inequality constraints

n = iteration number of decomposition algorithm

Parameters:

I = number of regions in time

J = number of finite elements in each region in time

K = number of collocation points in each finite element

N = number of realizations for process disturbances

M = number of realizations for parameter uncertainty

$\boldsymbol{\mathcal{A}}$ = matrix of orthogonal collocation weights

$\boldsymbol{f}$ = vector function of closed loop non-linear process model equations

$\boldsymbol{g}$ = vector function of inequality constraints

$\boldsymbol{h}$ = vector function of equality constraints

$\boldsymbol{\alpha}$ = infeasibility of inequality constraints $\boldsymbol{g}$ at each point in time

Φ_n = maximum infeasibility in iteration n

$\boldsymbol{\psi}$ = function to map the production sequence to a set-point profile

$\zeta^{\theta,\omega}$ = weight or probability of occurrence for realization (θ, ω)

t = time

Variables:

Δt_i = length of time region i

δt_i = length of every finite element in time region i

$\boldsymbol{x}(t)$ = vector of process states at time t

$\boldsymbol{x^{sp}}(t)$ = vector of process state set-points at time t

$\boldsymbol{u}(t)$ = vector of process inputs at time t

$\boldsymbol{y}(t)$ = vector of process outputs at time t

$\boldsymbol{x}_{ijk}$ = vector of process states in region i, finite element j, and collocation point k

$\boldsymbol{x}_{ijk}^{\theta,\omega}$= vector of process states in region i, finite element j, and collocation point k, corresponding to realization (θ, ω) of process disturbance and parameter uncertainty

$\boldsymbol{u}_{ijk}^{\theta,\omega}$= vector of process inputs in region i, finite element j, and collocation point k, corresponding to realization (θ, ω) of process disturbance and parameter uncertainty

$\boldsymbol{y}_{ijk}^{\theta,\omega}$= vector of process outputs in region i, finite element j, and collocation point k, corresponding to realization (θ, ω) of process disturbance and parameter uncertainty

$(\boldsymbol{y}^{sp})_{ijk}$= vector of process output set-points in region i, finite element j, and collocation point k

z = objective variable

$\boldsymbol{\kappa}$ = vector of design decisions

$\boldsymbol{\Lambda}$ = vector of control decisions

$\boldsymbol{\mathcal{B}}$ = binary matrix for sequence scheduling

$\boldsymbol{\eta}$ = vector of process disturbances

$\boldsymbol{\mathcal{P}}$ = vector of uncertain parameters

$\boldsymbol{\mathcal{D}}$ = vector of all design, control, and scheduling decisions $\{\boldsymbol{\kappa}, \boldsymbol{\Lambda}, \boldsymbol{\mathcal{B}}, \boldsymbol{\Delta t}\}$

$\boldsymbol{c}$ = set of critical realizations of process disturbance and parameter uncertainty

$\boldsymbol{\beta}$ = list of process set-points, in order of production

$\mathbf{Y^{sp}}$ = list of process output set-points, unordered

Figure Captions:

Figure 1: General production schedule of a multiproduct processing unit.

Figure 2: The time domain is discretized into I regions, where each region contains J finite elements, and each finite element contains K collocation points.

Figure 3: Decomposition algorithm proposed for integration of design, control and scheduling. The flexibility sub-problem returns the optimal design, control and scheduling scheme that can accommodate the realizations considered in the current critical set c. The feasibility problem identifies new critical realizations in the disturbances and uncertain parameters, and terminates if all considered realizations are feasible.

Figure 4: Schematic of CSTR system.

Figure 5: Concentration profile comparison between nominal operation (*Scenario A1*) and disturbed operation (*Scenario A2*). For the disturbed operation, the plot shows the responses due to the critical realization for process disturbance identified at the final iteration ($\omega=5$).

Figure 6: Concentration profile comparison between integrated method and sequential method.

Figure 7: (a) Reactor temperature profile for *Scenario B1* and *Scenario B2*; (b) Heat input profile from integrated method (*Scenario B1*).

Figure 8: Maximum infeasibility for temperature constraints identified by feasibility problem in each iteration n of the integrated approach.

Table 1: Previous works on Integration of Design, Control, and/or Scheduling

Topic	Authors	Contributions
Design & Control	Brengel and Seider, 1992	Fermentation process with model predictive control (MPC)
	Luyben and Floudas, 1994	Binary distillation with PI control
	Mohideen et al., 1996	Mixing tank and distillation column with PI control
	Kookos and Perkins, 2001	Evaporator and binary distillation with multiple PI controllers
	Bansal et al., 2002	Mixed-integer dynamic optimization of distillation with five PI controllers
	Seferlis and Georgiadis, 2004	Book, discussing many aspects of integration of design and control
	Ricardez Sandoval et al., 2008	Mixing tank with PI control using a robust modelling approach

	Sanchez-Sanchez and Ricardez-Sandoval, 2013	Single stage optimization of CSTR and ternary distillation with PI control
	Alvarado-Morales et al., 2010	Model-based optimization of bioethanol process
	Mansouri et al., 2016	Reactive distillation involving multiple elements
	Mehta and Ricardez-Sandoval, 2016	CSTR optimization using back-off approach and power series expansion (PSE)
	Ricardez-Sandoval et al., 2009; Sakizlis et al., 2004; Sharifzadeh, 2013; Vega et al., 2014; Yuan et al., 2012;	Reviews on integration of design and control
Control & Scheduling	Chatzidoukas et al., 2003	Optimal grade transitions for fluidized bed reactor with PI control
	Flores-Tlacuahuac and Grossmann, 2011	Non-isothermal PFR
	Zhuge and Ierapetritou, 2012	Multiproduct CSTR with PI control
	Engell and Harjunkoski, 2012	Review on integration of control and scheduling
	Chu and You, 2014b	Multiproduct CSTR with optimal control profile
	Chu and You, 2014c	Multiproduct CSTR with optimal control profile
	Zhuge and Ierapetritou, 2016	Methyl-methacrylate production with optimal control profile
Design & Scheduling	Bhatia and Biegler, 1996; Birewar and Grossmann, 1989; Castro et al., 2005; Heo et al., 2003; Lin and Floudas, 2001	Multiproduct design and scheduling of batch processes
Design, Control, & Scheduling	Terrazas-Moreno et al., 2008	Two stage optimization of methyl-methacrylate production with optimal control profile.
	Patil et al., 2015	Multiproduct process with disturbance and uncertainty, linearized process model, and frequency analysis.
	Pistikopoulos and Diangelakis, 2015	PAROC software for multi-parametric optimization. Summary of recent efforts towards integration of design, control, and scheduling.

Table 2: Summary of results from Scenario A

Operation Type	*Scenario A1*	*Scenario A2*
Optimal Process Cost ($)	177	388
CPU Time (s)	494	4,649 (four iterations)
Reactor Volume $V(L)$	13.6	15.4
Controller K_C, τ_i	1.95, 146	5.00, 346
ISE of concentration	1.22	17.63
Production sequence	A-B-C-E-D	A-C-E-D-B
Transition durations $\boldsymbol{\Delta t}$ (s)	46.2, 10.0, 18.3, 63.3, 10.0	33.9, 66.5, 119, 25.0, 46.6
Critical set c	$\boldsymbol{c} = \{(\omega = 0)\}$	$\boldsymbol{c} = \{(\omega = 0), (\omega = 5), (\omega = 2), (\omega = 4)\}$

Table 3: Uncertainty Realizations for Scenario B

Realization θ	Heat of Reaction $\Delta H_R\ (J/mol)$	Activation Energy $E_R\ (J/mol)$
0	5000	20000
1	6000	21000
2	4000	19000
3	4000	21000
4	6000	19000

Table 4: Summary of the flexibility analyses (*Scenario B1*)

Iteration	Critical Set	Solution	CPU Time	# of equations # of variables
1	$\boldsymbol{c}$ = {(0,0)}	V = 13.48 K_c, τ_i = 2.11, 823 Sequence: A-B-C-D-E $\boldsymbol{\Delta t}$ = 88, 52, 40, 48, 10	183 s	23,269 18,293
2	$\boldsymbol{c}$ = {(0,0), (8,1)}	V = 18.51 K_c, τ_i = 5.00, 130 Sequence: A-B-C-D-E $\boldsymbol{\Delta t}$ = 114, 10, 10, 10, 10	249 s	41,524 31,548
3	$\boldsymbol{c}$ = {(0,0), (8,1), (9,1)}	V = 18.54 K_c, τ_i= 5.00, 137 Sequence: A-B-C-D-E $\boldsymbol{\Delta t}$ = 101, 40, 10, 10, 10	469 s	59,779 44,803
4	$\boldsymbol{c}$ = {(0,0), (8,1), (9,1), (7,1)}	V = 18.56 K_c, τ_i= 5.00, 251 Sequence: A-B-E-D-C $\boldsymbol{\Delta t}$ = 52, 10, 99, 10, 10	1271 s	78,034 58,058
5	$\boldsymbol{c}$ = {(0,0), (8,1), (9,1), (7,1), (5,1)}	V = 18.89 K_c, τ_i = 5.00, 764 Sequence: A-B-E-D-C $\boldsymbol{\Delta t}$ = 155, 51, 281, 35, 28	920 s	96,289 71,313

Table 5: Summary of results from Scenario B.

Method	*Integrated approach (Scenario B1)*	*Sequential approach (Scenario B2)*	*Overdesign Sequential approach (Scenario B3)*
Optimal Process Cost ($)	607	385 (Infeasible)	735
Capital Cost ($)	189	150	225
Transition Cost ($)	110	27	119
Variability Cost ($)	308	208	391
CPU Time (s)	4,147 (5 iterations)	1,016 (sum of all stages)	801 (sum of all stages)
Reactor Volume $V(L)$	18.9	15.0	22.5
Controller K_C, τ_i	5.00, 764	5.00, 137	5.00, 456
Production sequence	A-B-E-D-C	A-B-D-E-C	A-C-B-E-D
Transition times $\boldsymbol{\Delta t}$ (s)	155, 51.0, 281, 35.4, 27.9	39.5, 20.9, 34.9, 10.1, 29.1	284, 178, 55.8, 48.4, 32.6
Critical set $\boldsymbol{c}$	$\boldsymbol{c} = \{(0,0), (8,1), (9,1), (7,1), (5,1), (9,3)\}$	Dynamically Infeasible	Dynamically Feasible

Table 6: Summary of results from Scenario C.

Method	*Increased Capital Cost Weight (Scenario C1)*	*Increased Scheduling Cost Weight (Scenario C2)*	*Increased Variability Cost Weight (Scenario C3)*
Total Process Cost ($)	626	618	638
Capital Cost ($)	208	189	189
Transition Cost ($)	110	121	110
Variability Cost ($)	308	308	339
Reactor Volume $V(L)$	18.9	18.9	18.9
Controller K_C, τ_i	5.00, 764	5.00, 765	5.00, 761
Production sequence	A-B-E-D-C	A-B-E-D-C	A-B-E-D-C
Transition times $\boldsymbol{\Delta t}$ (s)	155, 51.0, 281, 35.4, 27.9	155, 51.0, 281, 35.1, 27.3	155, 51.0, 281, 35.7, 28.2

Figure 1:

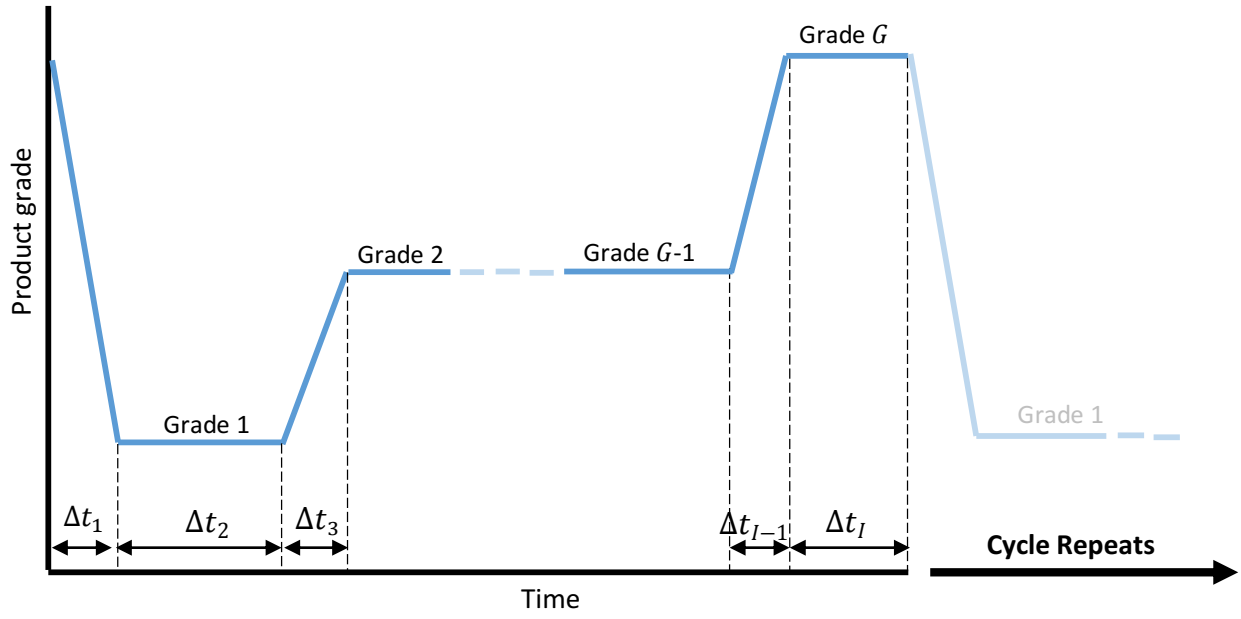

Figure 2:

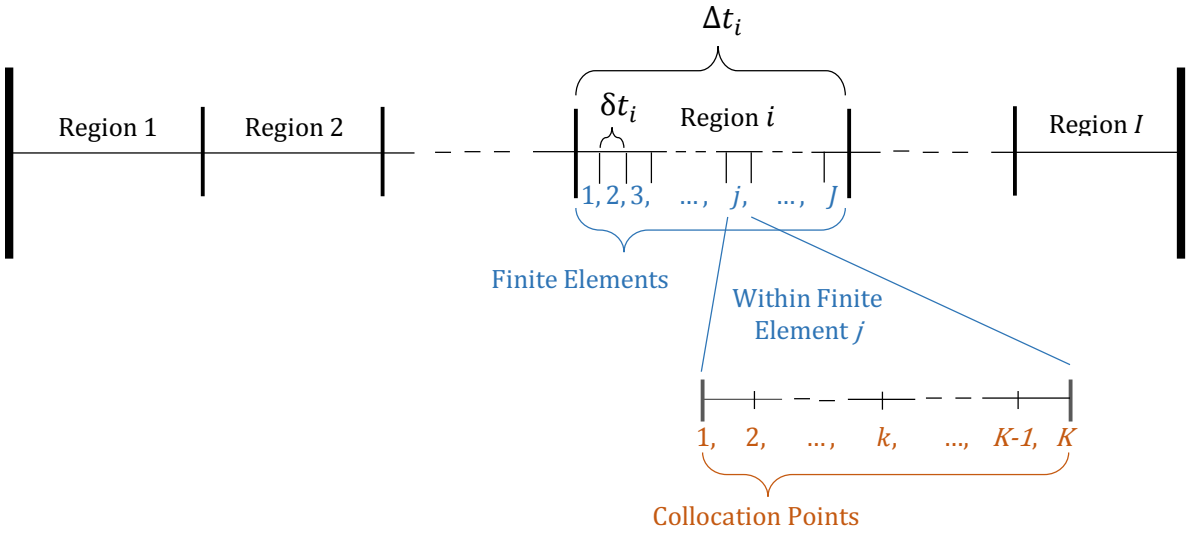

Figure 3:

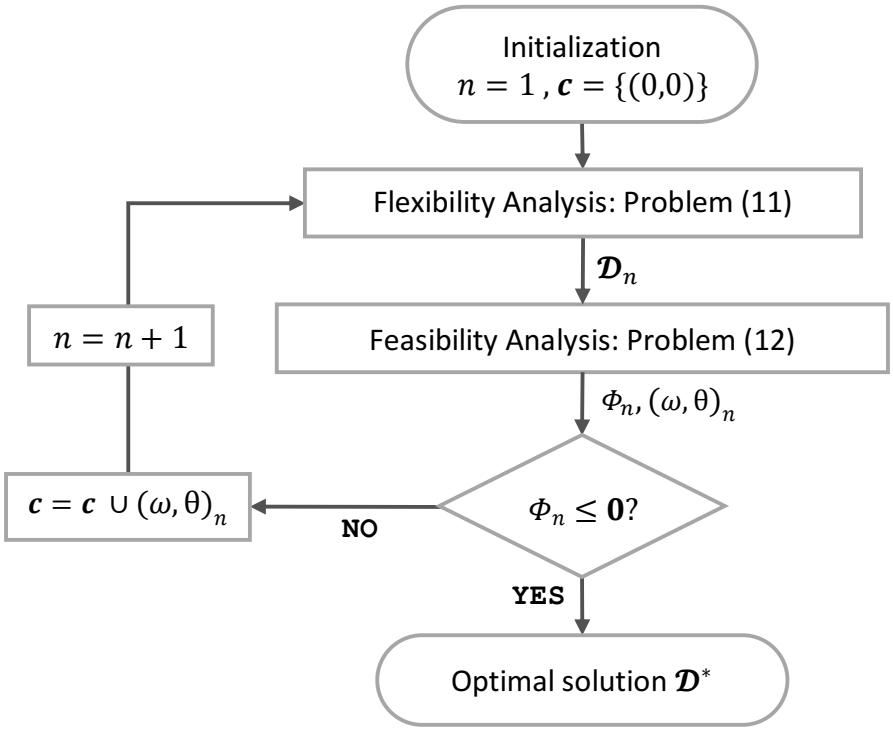

Figure 4:

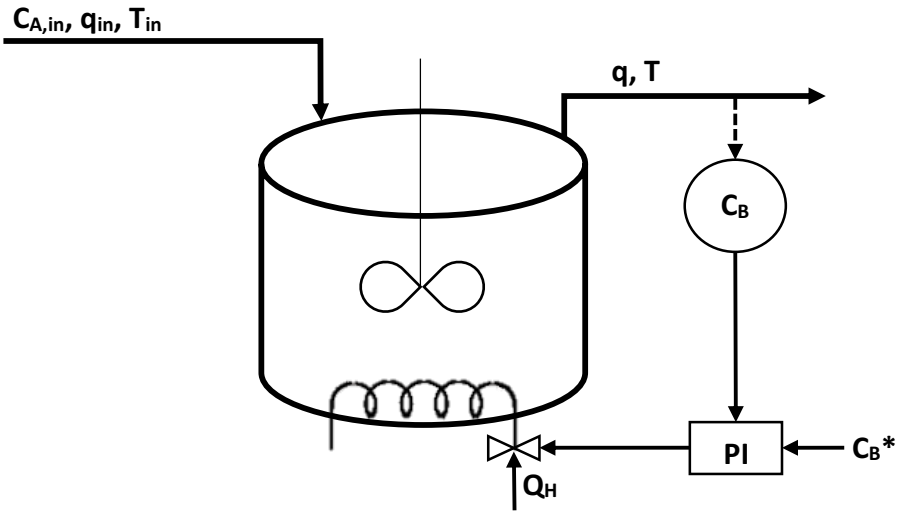

Figure 5:

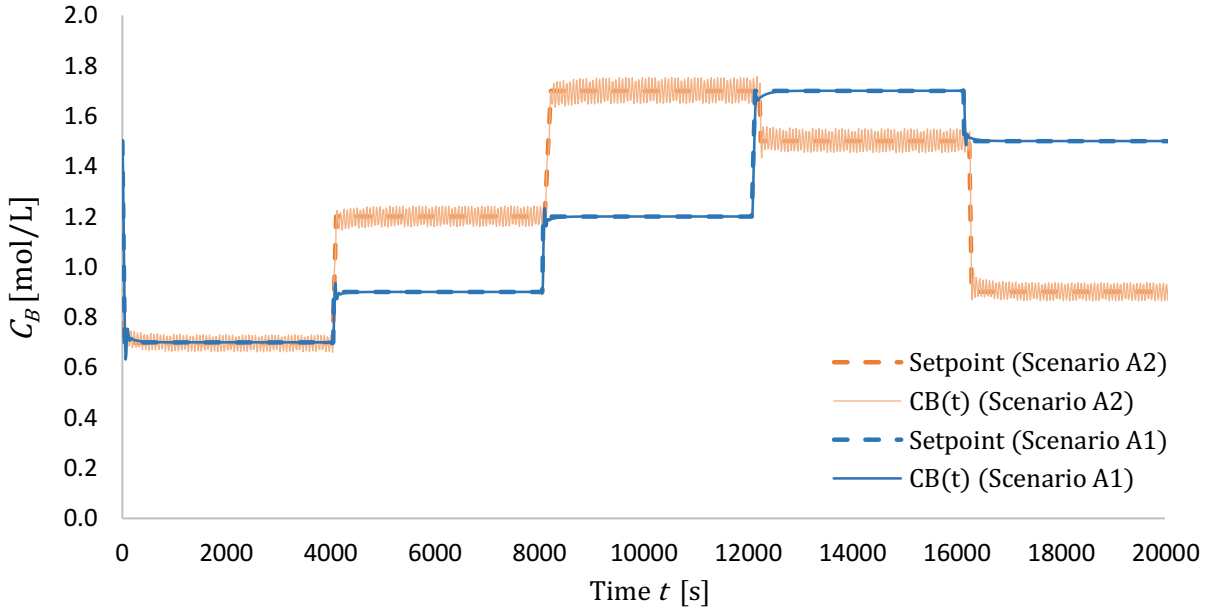

Figure 6:

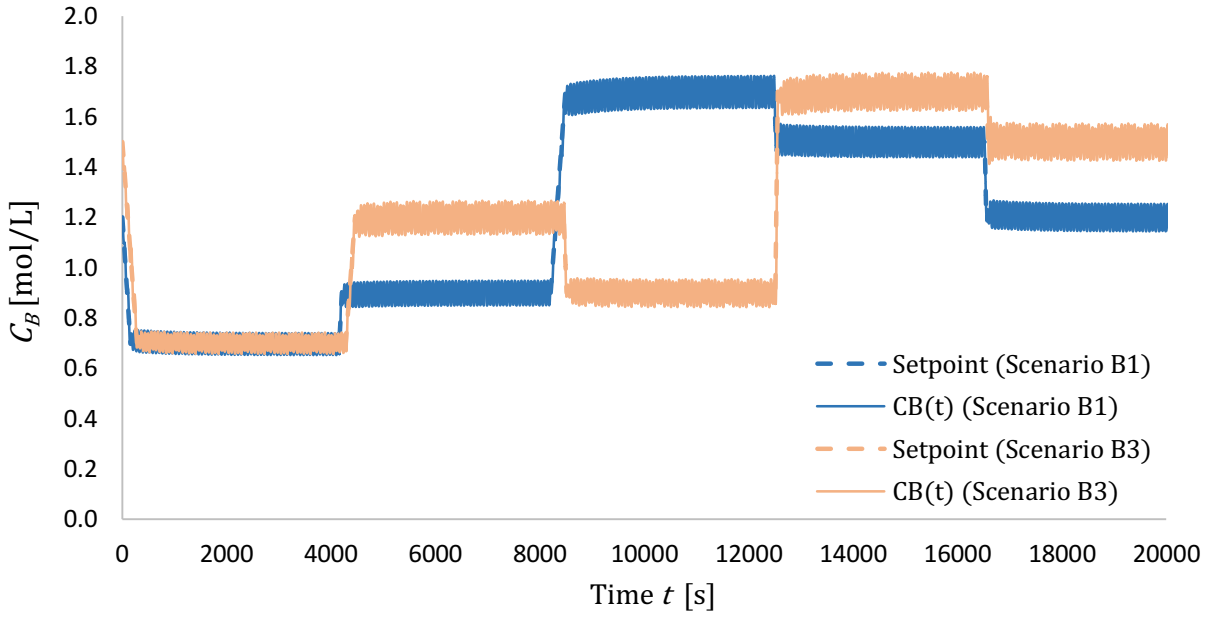

Figure 7:

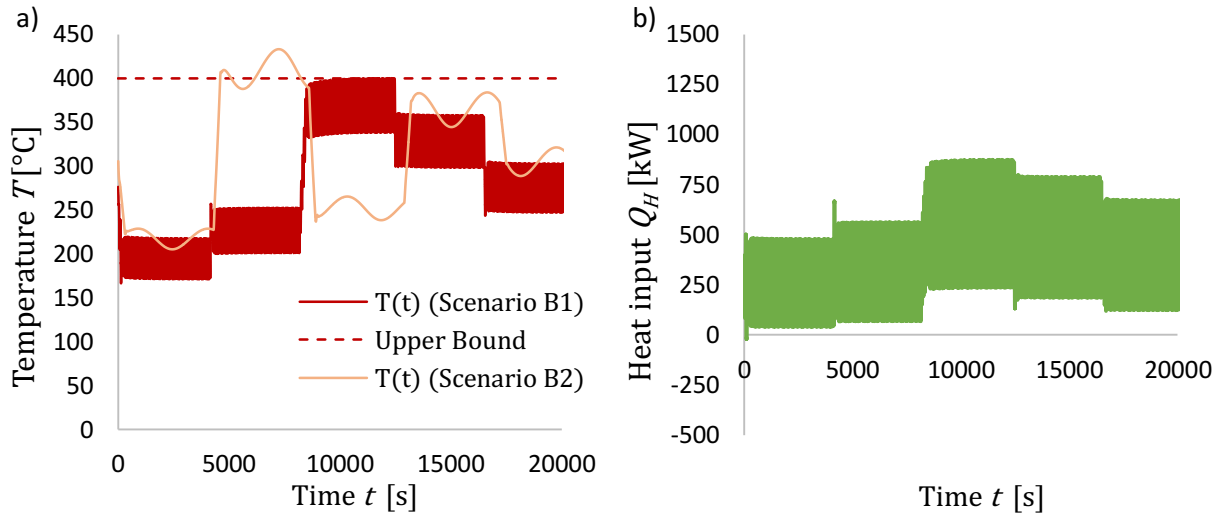

Figure 8: